1-1-2008

Short-term relationship of total electron content with geomagnetic activity in equatorial regions

X. Wang
University of Central Florida

Q. Sun

R. Eastes
University of Central Florida

B. Reinisch

C. E. Valladares

Short-term relationship of total electron content with geomagnetic activity in equatorial regions

X. Wang,[1,2] Q. Sun,[3] R. Eastes,[4] B. Reinisch,[5] and C. E. Valladares[6]

Received 27 November 2007; revised 4 July 2008; accepted 12 August 2008; published 8 November 2008.

[1] The short-term relationship between equatorial ionosphere and geomagnetic activity is examined. Hourly averages of the total electron content (TEC) and critical frequency of the F_2 layer (f_oF_2) are compared with the *Dst* index, a proxy for equatorial geomagnetic activity, at three local times (0700–0800, 1200–1300, and 1600–1700 LT) from March 1998 to August 1999. Owing to the geomagnetic latitude and local times used, positive storms, almost exclusively, are observed (cf. Prölss, 1995). While f_oF_2 measurements over an extended period (~10 years) have been studied (Matsushita, 1959) and TEC and f_oF_2 are coupled, TEC measurements can provide a significantly better signal-to-noise ratio. At timescales of 2–3, 3–5, 5–9, and 9–11 days, there are significant correlations (~0.4 at local noon, when all the data are included) between TEC and *Dst*. These correlations increase from morning to afternoon. By comparison, correlations between f_oF_2 and *Dst* are significantly smaller, ~0.2 (near the noise level) at local noon. Even during geomagnetically quiet times ($Dst > -20$), a clear correlation (0.21, which exceeds the 95% confidence level by 0.05) is seen between TEC and *Dst* at the shortest timescale examined. As geomagnetic activity increases, the correlations increase rapidly. For example, when moderate levels of geomagnetic activity ($Dst > -50$) are included for observations at local noon, distinct correlations (~0.3) are seen and persist for all but the longest timescale; with higher levels of geomagnetic activity included, there are distinct correlations at all the timescales examined. The presence of a significant correlation at quiet conditions and persistence of the correlation at moderate levels of activity are both unexpected.

Citation: Wang, X., Q. Sun, R. Eastes, B. Reinisch, and C. E. Valladares (2008), Short-term relationship of total electron content with geomagnetic activity in equatorial regions, *J. Geophys. Res.*, *113*, A11308, doi:10.1029/2007JA012960.

1. Introduction

[2] The ionosphere plays a central role in Earth's space weather. Day-to-day ionospheric variability is associated with strong coupling to the regions below and above. Owing to the limited availability of coincident data for the parameters influencing the ionosphere and the coupling within the Thermosphere-Ionosphere (T-I) system, understanding ionospheric density variations is difficult, but it is important for space weather specification and forecasting. A number of factors cause ionospheric variability. These factors include geomagnetic activity from above, as well as waves from below [*Forbes et al.*, 2000].

[3] It has long been appreciated that geomagnetic activity has short-term effects on the ionosphere [cf. *Rishbeth and Mendillo*, 2001]. Geomagnetic storm effects can last several days. At the equator ionospheric densities respond to changes in the neutral composition and to modifications of the equatorial anomaly by changes in both the neutral winds and the electric fields. Together, observations and theoretical modeling have helped us understand the ionospheric variations during geomagnetic storms, and excellent reviews of those works were presented by *Prölss* [1995] and *Mendillo* [2006]. As discussed by *Mendillo* [2006], the morphology and the physics of the ionosphere during storms are known and the most important issue is to improve the capacity of ionospheric modeling and forecasting.

[4] However, statistical analysis of extensive, long-term data sets is complicated by the occurrence of both positive and negative responses by the ionosphere. As *Matsushita* [1959] showed, there are common, global characteristics of *F* region storms: (1) The ionosphere has positive and negative responses, with the positive phase being more

[1]Department of Electrical and Computer Engineering, University of Central Florida, Orlando, Florida, USA.
[2]Now at INRIA Paris-Rocquencourt Research Centre, Rocquencourt, France.
[3]Department of Mathematics, University of Central Florida, Orlando, Florida, USA.
[4]Florida Space Institute, Department of Electrical and Computer Engineering, University of Central Florida, Orlando, Florida, USA.
[5]Department of Environmental, Earth and Atmospheric Sciences, University of Massachusetts, Lowell, Massachusetts, USA.
[6]Institute for Scientific Research, Boston College, Chestnut Hill, Massachusetts, USA.

0148-0227/08/2007JA012960

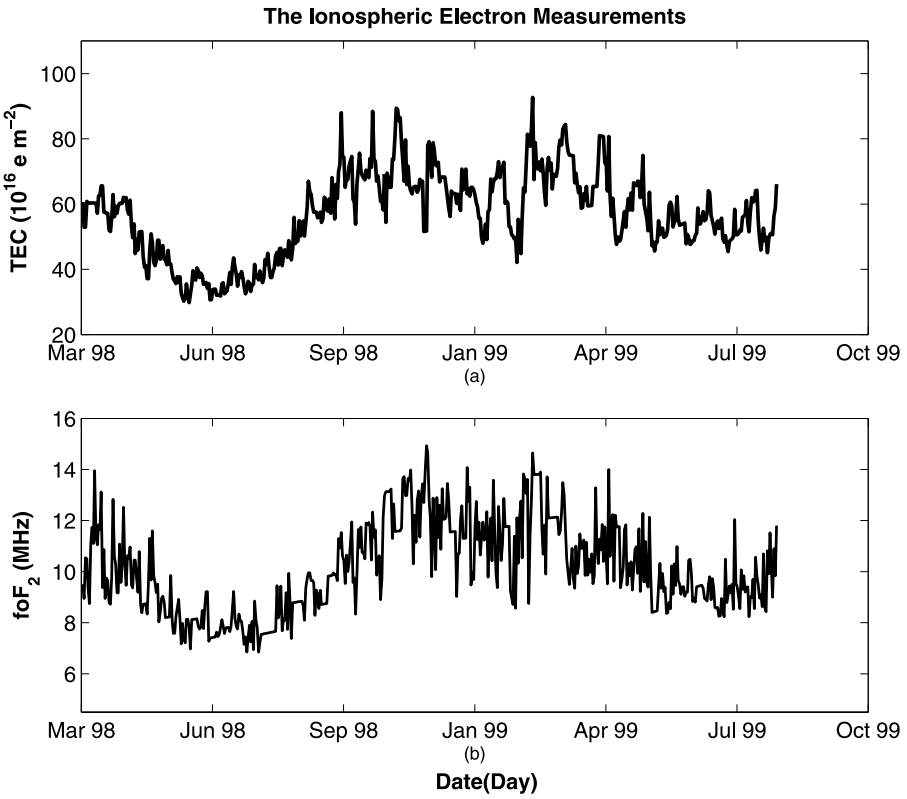

Figure 1. Total electron content (TEC) and f_oF_2 data at 1200–1300 LT from 1998 to 1999. (a) The TEC is from a GPS receiver in Ancon, Peru. (b) The f_oF_2 is from a Digisonde in Jicamarca, Peru.

prevalent at lower latitudes; (2) the positive phase has a noticeable local time component; its maximum amplitudes occur near 1800 LT at subauroral latitudes, earlier at higher latitudes, and later at lower latitudes; and (3) positive storms are more pronounced in winter, and negative storms are more pronounced in summer. *Prölss* [1995] summarized that at the equator the ionospheric response to storms is predominately positive in the daytime. Recent works by *Pirog et al.* [2006] and *Romanova et al.* [2006] found that, both in winter and summer seasons, the ionospheric disturbances are positive at low latitudes in the daytime. A positive response is also typical for lower levels of geomagnetic activity [*Hibberd and Ross*, 1967].

[5] Owing to the predominately positive response of the equatorial ionosphere, such observations are well suited for statistical analysis using wavelet methods [*Mallat*, 1989]. Previous studies [e.g., *Fagundes et al.*, 2005; *Grinsted et al.*, 2004; *Pancheva et al.*, 2003, 2004a, 2004b, 2006] have shown the power of wavelets in extracting short-term variations, using conventional two-band wavelets. In this paper multiband wavelets, which can decompose the data with finer resolutions and better reliability, are used. The accuracy of the multiband wavelets is studied, then they are used to examine the short-term relationships between ionospheric and geomagnetic data during almost two years of daily measurements.

[6] The goal of this study is to better understand the geomagnetic effects on the day-to-day ionospheric variations. While the *F*-layer peak electron densities were used in previous studies [e.g., *Rishbeth and Mendillo*, 2001; *Altadill and Apostolov*, 2003; *Wang et al.*, 2006], GPS receivers now measure the total electron content (TEC), an integrated electron density from the *D*, *E*, *F*, and topside regions. Total electron content measurements can provide significant insights to ionospheric physics on both global and local scales [*Mendillo*, 2006; *Mendillo and Klobuchar*, 2006]. *Wang et al.* [2006] found the TEC and *F*-layer peak density may respond differently to geomagnetic activity since the relationship between TEC and peak density can be affected by the changing scale heights (owing to the electron temperature variations in storm time).

[7] This study uses TEC measurements from a GPS receiver in Peru and coincident measurements of the peak electron density, the critical frequency of the F_2 layer (f_oF_2). These data are compared with the *Dst* index, an indicator of the equatorial geomagnetic activity. Three local hours of measurements (0700–0800, 1200–1300 and 1600–1700 LT) were analyzed to understand the local-time dependence of the ionosphere on geomagnetic activity. There is evidence that the ionospheric response depends on the geomagnetic activity level [*Mendillo and Schatten*, 1983]; therefore, the ionospheric response at three levels of geomagnetic activity ($Dst > -20$ or -50 and including all *Dst* levels) is also examined. The paper is presented in the following sequence: (1) data description, (2) data analysis (including the wavelet filters and correlation results), (3) discussion, and (4) conclusions.

2. Data

[8] Coincident observations of TEC and f_oF_2 from an equatorial location, as well as *Dst* index data are used in the

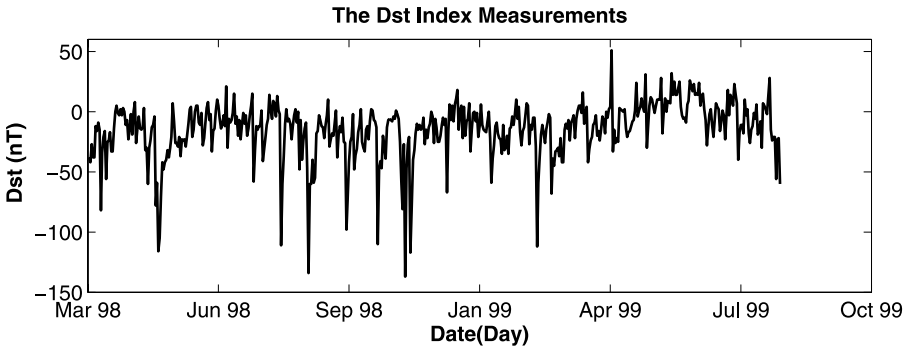

Figure 2. *Dst* measurements from 1998 to 1999.

analysis. The TEC data are from a GPS receiver [*Valladares et al.*, 2001] near Ancon, Peru (−77.15° longitude, −11.78° latitude, 1.47° geomagnetic latitude). Observations from March 1998 to August 1999 are used in this study. Hourly averages of TEC are calculated for all observations whose ionospheric pierce point occurred within −12 ± 2 degrees latitude and −77 ± 2 degrees longitude during the hour selected. The ionospheric pierce point, defined by intersection of the line of sight from GPS satellite to receiver with the peak of the *F* layer, is assumed to be 350 km. Possible errors from peak altitude variations are minimized by the use of near zenith (±2°) observations in this analysis. Averages of TEC measurements from the three local times (LTs) used (0700–0800 LT, 1200–1300 LT, and 1600–1700 LT) are calculated, and any gaps in the TEC data are filled using a cubic spline interpolation. An example of the TEC data, from 1200 to 1300 LT, is plotted in Figure 1a. The TEC decreases between March 1998 to June 1998 and increases to October 1998; then decreases slightly between March 1999 and July 1999. This variation is consistent with the annual anomaly, where the noon values of electron density are usually greater in December than in June.

[9] The f_oF_2 data are from a Digisonde at Jicamarca Radio Observatory in Peru [*Reinisch*, 1996]. The vertical soundings of the ionosphere are normally obtained every 15 or 30 min and were automatically scaled using the ARTIST inversion algorithm [*Reinisch and Xueqin*, 1983]. These data are downloaded from http://umlcar.uml.edu/DIDBase/, provided by the Center for Atmospheric Research at the University of Massachusetts, Lowell. There are usually 2–4 measurements in an hour, and all the measurements collected during an hour are used when calculating hourly averages. The local times and dates (0700–0800 LT, 1200–1300 LT, and 1600–1700 LT from March 1998 to August 1999) of the averaged f_oF_2 data match those of the TEC data. An example of f_oF_2 data at 1200–1300 LT is shown in Figure 1b.

[10] The *Dst* index is derived from magnetometer measurements at low latitudes and is an indicator of equatorial geomagnetic activity. Hourly *Dst* data were downloaded from the National Geophysical Data Center (http://ftp.ngdc.noaa.gov/STP/GEOMAGNETIC DATA/INDICES/DST/). An example of the *Dst* data, at 1200–1300 LT, is shown in Figure 2. Generally, values of −50 nT or less are indicative of a storm-level disturbance. Using this criterion there were 20 storms in the time period analyzed, as shown in Figure 2. Observations for the less disturbed *Dst* levels are also included in this study (e.g., deviations not exceeding −20 nT or −50 nT). Analysis of these lower levels of geomagnetic activity is unusually limited to atypical sets of observations [e.g., *Goncharenko et al.*, 2006].

3. Data Analysis

[11] The temporal variations in all three data series were separated using a set of tailored wavelet filters capable of providing high time resolution. Then cross correlations between the variations at each timescale were calculated in order to better understand their correspondence.

3.1. Wavelet Filters

[12] The three data series, TEC, f_oF_2, and *Dst* observations, were recorded in the time domain, with both the averages and differences having importance. The averages represent the long-term variations of signals, and the differences represent the variations over a short time period. Each can be represented using scaling and wavelet filters respectively. The scaling filter averages consecutive points, and the wavelet filters are Harr wavelets. Both are simple and easy to use, unlike some of the more complex wavelets [*Strang and Nguyen*, 1996]. The scaling and wavelet filters are expressed as

$$\text{Scaling filter} \qquad H_0 = [1 \;\; 1 \;\; 1], \tag{1}$$

$$\text{Wavelet filter 1} \qquad H_1 = \left[-\frac{\sqrt{2}}{2} \;\; \sqrt{2} \;\; -\;\; \frac{\sqrt{2}}{2}\right], \tag{2}$$

$$\text{Wavelet filter 2} \qquad H_2 = \left[-\frac{\sqrt{6}}{2} \;\; 0 \;\; -\;\; \frac{\sqrt{6}}{2}\right]. \tag{3}$$

[13] Wavelet transforms using these filters are implemented as "three-band" filter banks (i.e., three filters H_0, H_1, and H_2 are used at each level) as shown in Figure 3. Three levels of filter banks are shown in Figure 3 separated with down-samplers. The down-samplers select every third point; therefore, the results are only sensitive to events that are separated by three time steps. Scaling coefficients are generated by the H_0 filters, and wavelet coefficients (i.e., the wavelet transforms of the data) are generated by the H_1 and H_2 filters. The wavelet coefficients represent both the

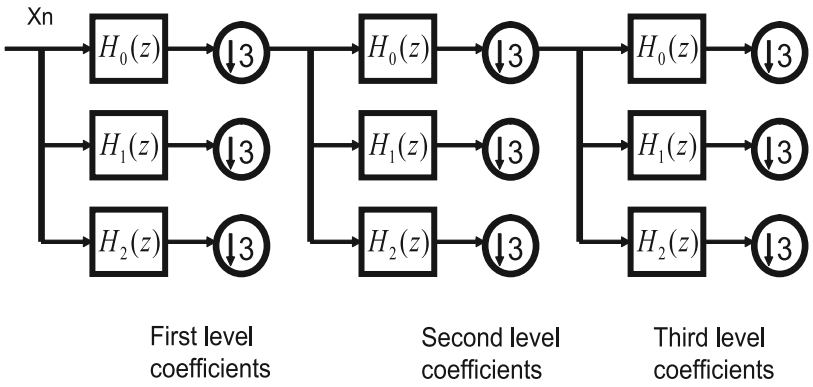

Figure 3. Three-band filter banks with three levels (only the analysis banks are shown).

frequencies and signal strengths in the data. Discussions of multiband wavelets and filter banks can be found in the work of *Vaidyanathan* [1993], *Strang and Nguyen* [1996], and *Sun et al.* [2001].

[14] In order to understand the ability of the wavelet filters to represent short-term variations in the data, the following tests are made: (1) sinusoidal signals with periods $\geq$2 days are input to the filter banks; (2) wavelet coefficients from each filter at each level are collected; and (3) power spectrum of the wavelet coefficients are examined using Welch's method. For each filter at each level, the magnitude of the power is integrated along the frequency spectrum (0 to 1) and the resulting magnitude is referenced as power in the following discussion. As the input periods change, the power extracted by each filter varies and the performance of the filters, that is, how well the filters can represent periodic signals, can be determined. For easier comparison, all the test inputs have the same magnitude, 1. All the power values are also scaled such that the largest power is represented by 1.

[15] The signal power captured by each wavelet filter is shown in Figure 4, for signals with 2 to 27 day periods. The wavelet filters can best extract the short-term variations with periods of 2–3, 3–5, 5–9, and 9–15 days. For example, the H_1 filter at the first level can extract most of the 2–3 day periods (0.5–0.8 of the total), and at the second level it extracts 0.4–0.6 of the 5–9 day periods. Therefore, the wavelet filters can be used to represent the short-term variations. As shown in Figure 4, the data are decomposed to four scales (2–3, 3–5, 5–9 and 9–15 days) from the first two levels, while only two scales (at ~2 and ~4 day, respectively) can be obtained from the same levels using the conventional two-band wavelets. (To get the same scales using two-band wavelets, four levels are necessary and less data would be used for the longer periods, resulting in less accurate results). Therefore, the three-band wavelets can provide an accurate representation of data variations in fine temporal resolution.

[16] However, the coefficients from the wavelet filters are affected by the longer periods. For example, the wavelet filter at the second level extracts not only the periods of 9–15 days but also 0.16–0.34 of the 16–23 day periods. In this study we focus on periods of $\leq$11 days owing to the analysis techniques employed and the same periods being used in previous studies of planetary wave signatures in f_oF_2 data [e.g., *Forbes et al.*, 2000; *Altadill and Apostolov*, 2003].

[17] In order to obtain a more accurate representation of shorter periods, removing the longer (>11 days) periods is desirable. This is accomplished by using Fourier transforms as a preprocessor [*Huang et al.*, 1998]. The Fourier transform is applied to the data, and the values of the longer periods are set to 0 then an inverse Fourier transform is applied. This method can also be used to remove the period overlaps between different wavelet filters seen in Figure 4. Since similar results are seen without applying the Fourier method to the overlaps, the results presented later are from removing the longer periods only. Therefore, used with the preprocessor, the wavelets can represent periods of 2–3, 3–5, 5–9, and 9–11 days.

3.2. Correlation Analysis and Results

[18] The TEC, f_oF_2 and *Dst* data are decomposed to timescales of 2–3, 3–5, 5–9 and 9–11 days. Then the relationships between geomagnetic activity and ionosphere

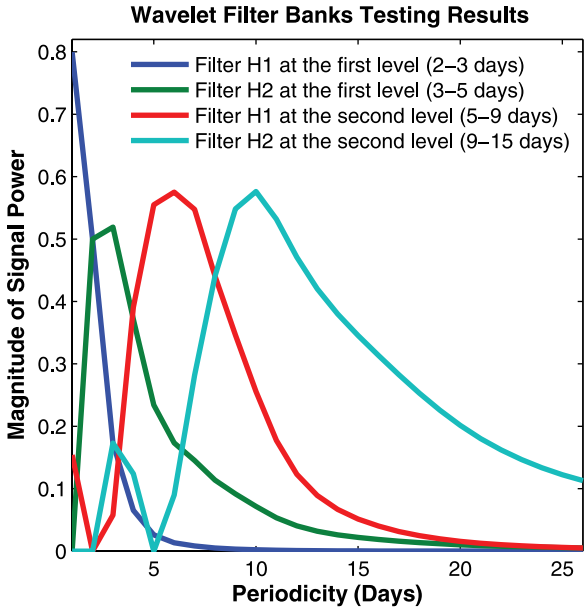

Figure 4. Frequency response of the wavelet filters. The wavelets can well represent short periods of 2–3, 3–5, 5–9, and 9–11 days.

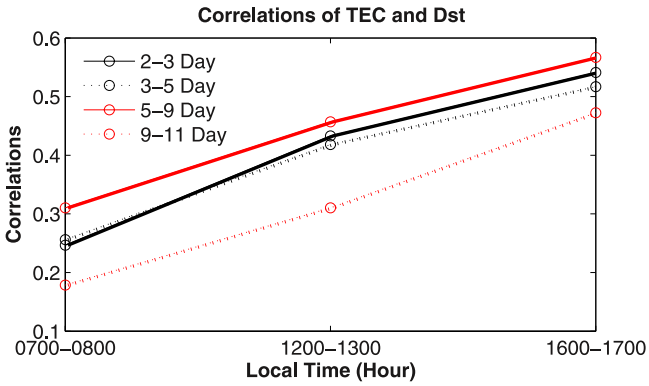

Figure 5. Correlations between *Dst* and TEC at Ancon, Peru, as a function of local time.

are evaluated for each scale using cross correlations. The *Dst* data used include the full range of geomagnetic activity.

[19] The cross correlations between TEC and *Dst* for each timescale at each local time (0700–0800 LT, 1200–1300 LT, and 1600–1700 LT) are shown in Figure 5. While the correlations between the ionosphere and *Dst* are negative, owing to *Dst* being negative, the magnitudes of correlations at each scale are used here.

[20] As shown in Figure 5, there are significant correlations between TEC and *Dst*, and similar diurnal trends are seen at all periods. The correlations range from 0.25 to 0.53 at a scale of 2–3 days, 0.25 to 0.51 at 3–5 days, 0.3 to 0.55 at 5–9 days, and 0.2 to 0.47 at 9–11 days. The 95% confidence level is 0.14 for the 2–3 and 3–5 days results, and it is 0.24 for 5–9 and 9–11 days results. The different confidence levels are due to selecting the third point at each level when using the down-samplers. All the correlations (except that for 9–11 day in the morning) exceed the confidence levels and the averaged correlation is as high as ~0.4.

[21] As seen in Figure 5, the correlations between the *Dst* and TEC increase from morning to afternoon. The increase is seen at all scales: 2–3, 3–5, 5–9, and 9–11 days. For example, at scales of 2–3 days, the correlation increases from 0.25 (in the morning) to 0.43 (at noon) and 0.53 (in the afternoon). To avoid possible effects from the prereversal enhancement that occurs just after sunset [*Farley et al.*, 1986; *Haerendel and Eccles*, 1992], measurements at 1600–1700 LT were presented in this study; however, 1700–1800 LT observations give similar results. This is consistent with positive disturbances observed in the equatorial regions during the main phase of most (~88%) magnetic storms at 0900–1800 LT [*Adeniyi*, 1986]. However, higher correlations are seen in the afternoon than at noon, presumably owing to local time variation of the neutral winds and electric fields.

[22] The correlations of f_oF_2 with *Dst* are also examined, using the same methods used for TEC and *Dst*. Typically, the correlations are ~0.2 lower for f_oF_2 than for TEC (but the confidence levels are similar, 0.14–0.24). An example, the correlations at local noon, is shown in Table 1. While the f_oF_2 represents peak electron densities at the F_2 layer, the TEC is integrated electron densities from the *D*, *E*, *F* (F_1 and F_2), and topside layers of atmosphere. Owing to the more limited volumes involved, the peak density is more sensitive than TEC is to coupling with lower and higher altitudes.

Table 1. Cross Correlations Between Local Noontime f_oF_2 and *Dst* From 1998 to 1999, With All Geomagnetic Conditions Included

Period, days	Correlation
2–3	0.2249
3–5	0.2016
5–9	0.2174
9–11	0.2509

4. Discussion

[23] Geomagnetic activity is often divided into quiet times, moderately disturbed times and storms. While most recent work has focused on storm times (*Dst* < −50) [e.g., *Buonsanto et al.*, 1992; *Buonsanto and Foster*, 1993; *Richards et al.*, 1994; *Richards*, 2002; *Field and Rishbeth*, 1997; *Basu et al.*, 2001; *Fuller-Rowell et al.*, 2002], the data used in this study include the full range of geomagnetic activity, including quiet and moderate conditions (*Dst* > −20 and −50). The correlations between TEC and *Dst* at different geomagnetic conditions at 1200–1300 LT are shown in Table 2 for each timescale, and a similar dependence on *Dst* is seen in the morning and evening observations. It is surprising that a significant correlation between TEC and *Dst* is seen even during quiet conditions. The other notable result is that significant correlations are seen for the longer periods at moderate levels of activity.

[24] As shown in Table 2, the correlation between TEC and geomagnetic activity increases with geomagnetic activity, as expected. What was not expected is the correlation above the 95% confidence level (by ~0.05) at the 2–3 day periods even during the quieter times (*Dst* > −20). This result indicates that even low levels of geomagnetic activity have a measurable effect on the equatorial TEC. While the cause of this correlation cannot be determined from these data, the 2–3 day period is close to the time period for recovery (~1 day) of the neutral winds (A. Burns, personal communication, 2008). Thermosphere-ionosphere general circulation model (TIEGCM) results may be useful for understanding whether neutral winds contribute significantly to the observed correlation. Previous work by *Altadill and Apostolov* [2003] found signatures of planetary waves with 2–3 day periods at higher latitudes (50°–60°) over Europe. If planetary waves are responsible for the observed correlations, this suggests their effects are more significant at the equator than would

Table 2. Cross Correlations Between TEC and *Dst* at Noontime Under Different Geomagnetic Conditions

Period, days	*Dst* > −20	*Dst* > −50	*Dst* All
2–3	0.21545	0.36864	0.43005
3–5	0.15581	0.30953	0.41464
5–9	0.14066	0.30759	0.45501
9–11	0.16629	0.19556	0.3029

be expected from the work at higher latitudes, or that their effects on TEC are more significant. *Altadill and Apostolov* [2003] saw signatures of planetary waves with 2–3 days in 12% of the days. Assuming the planetary wave signatures can be seen for the 3 days after being produced, there would be events producing these waves on 4% of the days. This corresponds approximately to the number of storms (20 in the ~500 days used in this study) with $Dst < -50$ during the observations analyzed here. However, significant correlations are seen for all three levels of *Dst* considered (Table 2), indicating the source of the 2–3 day correlations occurs much more frequently than during geomagnetic storms with $Dst < -50$.

[25] More distinct correlations are seen when days with moderate geomagnetic activity are included. When all data for which $Dst > -50$ are included, at the 2–3 day scale a correlation of 0.37 is seen, and a 0.3 correlation is seen at both 3–5 and 5–9 day scales. The effects of moderate activity ($Dst > -50$) seem to persist for ~10 days, significantly longer than the timescales for the neutral winds. Atmospheric waves may play a significant role in the persistence of the correlations. Recent studies have suggested geomagnetic activity can be responsible for at least 0.2–0.3 of the total planetary wave signatures in the midlatitude *F* region in the periods of 5–10 days [*Altadill and Apostolov*, 2003; *Fagundes et al.*, 2005]. Planetary wave activity would force the ions and consequently affect the electric fields and the ionosphere.

5. Conclusions

[26] Hourly averages of the Total Electron Content (TEC) and critical frequency of the F_2 layer (f_oF_2) from one and a half years (March 1998 to August 1999) of observations at an equatorial station in the American sector are compared with *Dst*, a proxy for the equatorial geomagnetic activity, at three local times (0700–0800 LT, 1200–1300 LT and 1600–1700 LT). Comparisons are made for data that include the full range of geomagnetic activity, and for data limited to quiet and moderate conditions ($Dst > -20$ and -50). Although no attempt was made to separate positive and negative storms, most of the storms (~90%) are positive, as expected for an equatorial station, and the analysis concentrates on the recovery period, during which a positive response is expected. When all the data are included, the correlations increase from morning to afternoon, and comparisons of data with periods of 2–3, 3–5, 5–9 and 9–11 days show significant correlations between TEC and *Dst*. Even for somewhat quiet conditions, $Dst > -20$, correlations clearly above the 95% confidence level (by ~0.05 at noon) are seen between *Dst* and TEC at periods of 2–3 days. Significant correlations at 2–3 day periods are seen for all the levels of geomagnetic activity examined. While such variations are often attributed to planetary waves, studies of the midlatitude ionosphere [e.g., *Altadill and Apostolov*, 2003] find planetary wave effects are significantly less prevalent than is seen in the equatorial observations analyzed in this paper.

[27] Under moderately disturbed conditions ($Dst > -50$), significant correlations can be seen for even longer periods examined. While the correlations vary with local times as the neutral winds do, this persistence could be a consequence of the planetary wave activity which reportedly results from geomagnetic activity [cf. *Altadill and Apostolov*, 2003; *Fagundes et al.*, 2005]. However, if planetary waves are responsible, their effects are more significant over South American than is expected from the previous analyses of data from midlatitudes. While the neutral winds also respond to geomagnetic activity, their recovery time is expected to be shorter than the periods studied (A. Burns, personal communication, 2008). Although further analysis is necessary to understand the observed relationship between TEC and *Dst*, the correlations clearly represent a significant portion of the observed TEC variation.

[28] **Acknowledgments.** The work at the University of Central Florida was supported by NASA grant NAG5–13507. The work at Boston College was also partially supported by Air Force Research Laboratory contract F19628-02-C-0087, AFOSR task 2311AS. The observatory of Ancon is operated by the Geophysical Institute of Peru, Ministry of Education. B. W. R. was supported by AF grant FA718-06-0072. The authors are grateful to Alan Burns for sharing his knowledge of the neutral winds in the Earth's atmosphere. The authors thank the reviewers for their comments.

[29] Amitava Bhattacharjee thanks Paulo Camargo and another reviewer for their assistance in evaluating this paper.

References

Adeniyi, J. O. (1986), Magnetic storm effects on the morphology of the equatorial F2-layer, *J. Atmos. Sol. Terr. Phys.*, *48*, 695–702, doi:10.1016/0021-9169(86)90019-X.

Altadill, D., and E. Apostolov (2003), Time and scale size of planetary wave signatures in the ionospheric *F* region: Role of the geomagnetic activity and mesosphere/lower thermosphere winds, *J. Geophys. Res.*, *108*(A11), 1403, doi:10.1029/2003JA010015.

Basu, S., S. Basu, K. M. Groves, H.-C. Yeh, S.-Y. Su, F. J. Rich, P. G. Sultan, and M. J. Keskinen (2001), Response of the equatorial ionosphere in the South Atlantic region to the great magnetic storm of July 15, 2000, *Geophys. Res. Lett.*, *28*(18), 3577–3580.

Buonsanto, M. J., and J. C. Foster (1993), Effects of magnetospheric electric fields and neutral winds on the low-middle latitude ionosphere during the March 20–21, 1990, storm, *J. Geophys. Res.*, *98*, 19,133–19,140.

Buonsanto, M. J., J. C. Foster, and D. P. Sipler (1992), Observations from Millstone Hill during the geomagnetic disturbances of March and April 1990, *J. Geophys. Res.*, *97*, 1225–1243.

Fagundes, P. R., V. G. Pillat, M. J. A. Bolzan, Y. Sahai, F. Becker-Guedes, J. R. Abalde, and S. L. Aranha (2005), Observations of *F* layer electron density profiles modulated by planetary wave type oscillations in the equatorial ionospheric anomaly region, *J. Geophys. Res.*, *110*, A12302, doi:10.1029/2005JA011115.

Farley, D., E. Bonelli, B. Fejer, and M. Larsen (1986), The prereversal enhancement of the zonal electric field in the equatorial ionosphere, *J. Geophys. Res.*, *91*, 13,723–13,728.

Field, P. R., and H. Rishbeth (1997), The response of the ionospheric F2-layer to geomagnetic activity: An analysis of worldwide data, *J. Atmos. Sol. Terr. Phys.*, *59*(2), 163–180, doi:10.1016/S1364-6826(96)00085-5.

Forbes, J. M., S. E. Palo, and X. Zhang (2000), Variability of the ionosphere, *J. Atmos. Sol. Terr. Phys.*, *62*, 685–693, doi:10.1016/S1364-6826(00)00029-8.

Fuller-Rowell, T. J., G. H. Millward, A. D. Richmond, and M. V. Codrescu (2002), Storm-time changes in the upper atmosphere at low latitudes, *J. Atmos. Sol. Terr. Phys.*, *64*(12–14), doi:10.1016/S1364-6826(02)00101-3.

Goncharenko, L., et al. (2006), Large variations in the thermosphere and ionosphere during minor geomagnetic disturbances in April 2002 and their association with IMF B_y, *J. Geophys. Res.*, *111*, A03303, doi:10.1029/2004JA010683.

Grinsted, A., J. C. Morre, and S. Jevrejeva (2004), Application of the cross wavelet transform and wavelet coherence to geophysical time series, *Nonlinear Processes Geophys.*, *11*, 561–566.

Haerendel, G., and V. Eccles (1992), The role of the equatorial electrojet in the evening ionosphere, *J. Geophys. Res.*, *97*, 1181–1192.

Hibberd, F. H., and W. J. Ross (1967), Variations in total electron

content and other ionospheric parameters associated with magnetic storms, *J. Geophys. Res.*, *72*, 5331–5337.

Huang, N. E., Z. Shen, and S. R. Long (1998), The empirical mode decomposition method and the Hilbert spectrum for nonlinear and non-stationary time series analysis, *Proc. R. Soc. London, Ser. A*, *454*, 903–995.

Mallat, S. G. (1989), A theory of multiresolution signal decomposition: The wavelet representation, *IEEE Trans. Pattern Anal. Mach. Intel.*, *11*, 647–693, doi:10.1109/34.192463.

Matsushita, S. (1959), A study of the morphology of ionospheric storms, *J. Geophys. Res.*, *64*, 305–321.

Mendillo, M. (2006), Storms in the ionosphere: Patterns and processes for total electron content, *Rev. Geophys.*, *44*, RG4001, doi:10.1029/2005RG000193.

Mendillo, M., and J. A. Klobuchar (2006), Total electron content: Synthesis of past storm studies and needed future work, *Radio Sci.*, *41*, RS5S02, doi:10.1029/2005RS003394.

Mendillo, M., and K. Schatten (1983), Influence of solar sector boundaries on ionospheric variability, *J. Geophys. Res.*, *88*(A11), 9145–9153.

Pancheva, D., C. Haldoupis, C. E. Meek, A. H. Manson, and N. J. Mitchell (2003), Evidence of a role for modulated atmospheric tides in the dependence of sporadic E layers on planetary waves, *J. Geophys. Res.*, *108*(A5), 1176, doi:10.1029/2002JA009788.

Pancheva, D., et al. (2004a), Variability of the quasi-2-day wave observed in the MLT region during the PSMOS campaign of June–August 1999, *J. Atmos. Sol. Terr. Phys.*, *66*, 539–565, doi:10.1016/j.jastp.2004.01.008.

Pancheva, D., N. J. Mitchell, and P. T. Younger (2004b), Meteor radar observations of atmospheric waves in the equatorial mesosphere/lower thermosphere over Ascension Island, *Ann. Geophys.*, *22*, 387–404.

Pancheva, D., et al. (2006), Two-day wave coupling of the low-latitude atmosphere-ionosphere system, *J. Geophys. Res.*, *111*, A07313, doi:10.1029/2005JA011562.

Pirog, O. M., N. M. Polekh, A. V. Tashchilin, E. B. Romanova, and G. A. Zherebtsov (2006), Response of ionosphere to the great geomagnetic storm of September 1998: Observation and modeling, *Adv. Space Res.*, *37*(5), 1081–1087, doi:10.1016/j.asr.2006.02.005.

Prölss, G. W. (1995), Ionospheric *F* region storms, in *Handbook of Atmospheric Electrodynamics*, vol. II, edited by H. Volland, pp. 195–247, CRC Press, Boca Raton, Fla.

Reinisch, B. W. (1996), Modern ionosondes, in *Modern Ionospheric Science*, edited by H. Kohl, R. Rüster, and K. Schlegel, pp. 440–458, Eur. Geophys. Soc., Katlenburg-Lindau, Germany.

Reinisch, B. W., and H. Xueqin (1983), Automatic calculation of electron density profiles from digital ionograms: 3. Processing of bottomside ionograms, *Radio Sci.*, *18*, 477–492.

Richards, P. G. (2002), Ion and neutral density variations during ionospheric storms in September 1974: Comparison of measurement and models, *J. Geophys. Res.*, *107*(A11), 1361, doi:10.1029/2002JA009278.

Richards, P. G., D. G. Torr, M. J. Buonsanto, and D. P. Sipler (1994), Ionospheric effects of the March 1990 magnetic storm: Comparison of theory and measurement, *J. Geophys. Res.*, *99*(A12), 23,359–23,365.

Rishbeth, H., and M. Mendillo (2001), Patterns of F2-layer variability, *J. Atmos. Sol. Terr. Phys.*, *63*, 1661–1680, doi:10.1016/S1364-6826(01)00036-0.

Romanova, E. B., A. V. Tashchilin, G. A. Zherebtsov, O. M. Pirog, N. M. Polekh, V. F. Smirnov, A. E. Stepanov, S. S. Jiankui, and W. Xiao (2006), Modeling of the seasonal effects of geomagnetic storms in the eastern Asian ionosphere, *Int. J. Geomagn. Aeron.*, *6*, GI3004, doi:10.1029/2005GI000119.

Strang, G., and T. Q. Nguyen (1996), *Wavelets and Filter Banks*, Wellesley Coll., Wellesley, Mass.

Sun, Q., N. Bi, and D. Huang (2001), *An Introduction to Multiband Wavelets*, Zhejiang Univ. Press, Zhejiang, China.

Vaidyanathan, P. P. (1993), *Miltirate Systems and Filter Banks*, Prentice-Hall, Upper Saddle River, N. J.

Valladares, C. E., S. Basu, K. Groves, M. P. Hagan, D. Hysell, A. J. Mazzella, and R. E. Sheehan (2001), Measurement of the latitudinal distributions of total electron content during equatorial spread *F* events, *J. Geophys. Res.*, *106*(A12), 29,133–29,152.

Wang, W., A. G. Burns, and T. L. Killeen (2006), A numerical study of the response of ionospheric electron temperature to geomagnetic activity, *J. Geophys. Res.*, *111*, A11301, doi:10.1029/2006JA011698.

R. Eastes, Florida Space Institute, Department of Electrical and Computer Engineering, University of Central Florida, Orlando, FL 32816, USA.

B. Reinisch, Department of Environmental, Earth and Atmospheric Sciences, University of Massachusetts, Lowell, MA 01854, USA.

Q. Sun, Department of Mathematics, University of Central Florida, Orlando, FL 32816, USA.

C. E. Valladares, Institute for Scientific Research, Boston College, Chestnut Hill, MA 02467, USA.

X. Wang, INRIA Paris-Rocquencourt Research Centre, Domaine de Voluceau-Rocquencourt, 78153 Le Chesnay Cedex, France. (shannon_ucf@hotmail.com)